Receiver Placement and Number Selection of Ground-Based Integrity Monitor Via Convex Optimization

Yu-Fang Lai, Juan Blanch, Todd Walter
Stanford University

BIOGRAPHY

Yu-Fang Lai is a Ph.D. candidate at Stanford GPS Lab. He received Bachelor's degree in Aero/Astro from National Cheng-Kung University in 2020, and Master's degree in Aero/Astro from Stanford in 2022.
Juan Blanch is a senior research engineer at Stanford University. He is a graduate of Ecole Polytechnique in France, he holds an M.S. degree in electrical engineering and a Ph.D. degree in aeronautics and astronautics from Stanford University.
Todd Walter is a Professor at Stanford University and the faculty of Stanford GPS Lab. He received his B.S. degree in physics from Rensselaer Polytechnic Institute and his Ph.D. degree in 1993 from Stanford University.

ABSTRACT

In this paper, we address the issue of designing the geometric relations of a ground-based integrity monitor system. Specifically, where the receivers should be placed; how many receivers are needed. The problem of determining the locations of the receivers is formulated as a convex optimization problem, where the locations of the receivers are determined by indirectly minimizing the protection levels of the target users. It is demonstrated that the number of receiver numbers is straightforward to be determined. The design results from the convex optimization is compared with an existing monitor network with a size of 56 stations and demonstrate the impact of different numbers of reference receivers to the performance of the network using almanac data. This work supports designing, selecting and placing reference stations when designing monitor networks.

I. INTRODUCTION

Precise Point Positioning (PPP) is a positioning technique that can achieve decimeter level of positioning accuracy for kinematic users of Global Navigation Satellite System (GNSS), and centimeter level for static users, with only the code and carrier phase pseudorange measurements. The extremely accurate positioning results rely on the sophisticated modeling of the pseudorange errors (Zumberge et al., 1997), and the use of precise corrections such as precise satellite clock bias and precise ephemeris. The modeling of the pseudorange errors include but are not limited to: atmospheric effects, antenna phase biases, antenna phase variations, differential code bias, solid earth tides, gravitational deformation and etc. In addition to error modeling, PPP also considers temporal correlations and the prior of the models when estimating the user position. The typical approach of realizing PPP standard utilizes Extended-Kalman Filter (EKF) (Welch et al., 1995) to estimate the user position and the associated pseudorange errors. In addition to the error modelings, which can be accomplished independently in a standalone GNSS receiver, the precise corrections the PPP users apply are entirely reliant on the service providers. Without the precise satellite clock and precise ephemeris, the accuracy of the positioning result degrades to 1-3 m if using the navigation message broadcast in the GNSS signals. The integrity and the accuracy of PPP users therefore completely rely on the precise correction information the PPP service providers broadcast.

In the previous works Lai et al. (2026), we demonstrated that the performance of the integrity monitor (Lai et al., 2024) can be evaluated as the user protection levels at steady-state at anywhere on Earth. An approximate form of steady-state information filter is derived, and it decoupled the contribution of each reference receiver towards the estimation of the uncertainty of the satellite clock and ephemeris errors, i.e. the estimate of the covariance of URE from the fault-tolerant filter, into per receiver contribution. This allows extremely fast computation of the URE covariance at steady-state. Therefore, make it possible to iterate through different combinations of receivers by evaluating the performance at different user locations or even globally.

In this paper, we extend upon the steady-state information form of the satellite errors derived from the previous work and formulate the problem of receiver placement into a form of sensor selection as described in Lai et al. (2026). First, we identify the candidate locations of the reference receivers for the monitoring network. The total number can be as many as hundreds of receivers scattered worldwide. Then, we select a fixed number of receivers from the pool of candidate receivers such that the protection levels of the target users are minimized. The whole selection process is formulated as a single constraint convex optimization problem. In the example we demonstrated, we can select 56 reference stations out of the total number of 200

candidate reference stations. It is shown that the result of the new 56 stations outperforms the old 56 stations network, which is manually chosen and involves unreliable heuristics. With the ability to optimally determine the geometry of a fixed number of the receivers, the number of the receivers a network requires is straightforward. The greater number of receivers are included in a network, the better the performance. As a result, one only needs to incrementally or decrementally change the size of the network upon each design of the receiver selection, and then evaluate the performance of such network to verify if the design is satisfactory.

In addition to formulating the convex optimization problem, a new design of network from uniformly distributed candidate receivers is obtained from the design process described in this paper and compared with an existing receiver network shown in Lai et al. (2026) to demonstrate the effectiveness of designing the network as a optimization problem.

This paper is structured as follows: Sec.II formulates measurement models of the IMS and PPP users and introduces the integrity information used by the users. Sec.III explains the use of steady-state Kalman and Information filter and derives derive the steady-state approximation of the covariance of the satellite errors that can greatly reduce the computation. Sec.IV introduces the dataset used in this paper. Sec.V shows the global steady-state VPL from actual receiver network, simulated data with almanac, and the baseline percentage of the actual and simulated VPL. Finally, Sec.VI concludes the paper.

II. BACKGROUND

1. Measurement Models of PPP Users

$$\rho_{\text{IF},r}^{(k)} = \| \overrightarrow{x}_{sat}^{(k)} - \overrightarrow{x}_{pos,r} \| + \left(b_r - b_{sat}^{(k)} \right) + m_r^{(k)} \nabla \hat{T}_r + R_{\rho,r}^{(k)} + \epsilon_r^{(k)} \tag{1}$$

$$\phi_{\text{IF},r}^{(k)} = \| \overrightarrow{x}_{sat}^{(k)} - \overrightarrow{x}_{pos,r} \| + \left(b_r - b_{sat}^{(k)} \right) + m_r^{(k)} \nabla \hat{T}_r + A_r^{(k)} + R_{\phi,r}^{(k)} + \epsilon_r^{(k)} \tag{2}$$

Eq.1 and Eq.2 are the dual-frequency ionospheric free combination of code-phase and carrier-phase pseudorange models from the kth satellite at r^{th} receiver in Earth-Center Earth-Fixed (ECEF) coordinate, respectively. $\overrightarrow{x}_s^{(k)} \in \mathbb{R}^{3\times 1}$ is the ephemeris, $\overrightarrow{x}_{pos,r}$ is the position of the receiver, b_r is the receiver clock bias, $b_{sat}^{(k)}$ is the satellite clock bias, $m_r^{(k)}$ is the mapping function for the tropospheric delay, $\nabla \hat{T}_r$ is the wet delay error, and $A_r^{(k)}$ si the floating ambiguities. $R_\rho^{(k)}$ and $R_\phi^{(k)}$ consist of all the modeled effects for code and carrier phase respectively, including satellite antenna phase center offset, satellite/receiver antenna phase variation, relativistic effects, solid earth tide modeling, ocean loading, modeled tropospheric delay, Sagnac Effect, group delay variation for code phase measurements and phase wind up for carrier phase measurements. Finally, $\epsilon_r^{(k)}$ is all the un-modeled effects to the measurement models and is assumed to be normally distributed. Eq.1 and Eq.2 are the measurement models used PPP users adopt in this paper.

Therefore, we can define the state vector of a single GNSS receiver as:

$$\overrightarrow{x_r} = \begin{bmatrix} b_r \\ \nabla b_r \\ \nabla \hat{T}_r \\ A_r^{(1)} \\ \vdots \\ A_r^{(k)} \end{bmatrix} \tag{3}$$

given that the receivers are static and the positions are known parameters.

2. Measurement Models of Fault-Tolerant Filter

$$\rho_{\text{IF},r}^{(k)} = \| \overrightarrow{x}_{sat}^{(k)} - \overrightarrow{x}_{pos,r} + \Delta \overrightarrow{\gamma}^{(k)} \| + \left(b_r - b_{sat}^{(k)} \right) + m_r^{(k)} \nabla \hat{T}_r + R_{\rho,r}^{(k)} + \zeta^{(k)} + \epsilon_r^{(k)} \tag{4}$$

$$\phi_{\text{IF},r}^{(k)} = \| \overrightarrow{x}_{sat}^{(k)} - \overrightarrow{x}_{pos,r} + \Delta \overrightarrow{\gamma}^{(k)} \| + \left(b_r - b_{sat}^{(k)} \right) + m_r^{(k)} \nabla \hat{T}_r + A_r^{(k)} + R_{\phi,r}^{(k)} + \zeta^{(k)} + \epsilon_r^{(k)} \tag{5}$$

Eq.4 and Eq.5 are the measurement models of the fault-tolerant filter operated in the IMS. They are similar to Eq.1 and Eq.2 except the additional error states, $\zeta^{(k)}$ and $\Delta \overrightarrow{\gamma}^{(k)}$, that account for the satellite clock errors and ephemeris errors, respectively. These two states are assumed without any prior and reset to zero at each time-update with their process noise as large as the

receiver clock bias states. This is reflecting the fact that we have no prior knowledge about when and what type of satellite clock and ephemeris faults can occur. It is shown in Lai et al. (2024) that this formulation can accurately capture the satellite faults in the range domain at the potential user locations.

The state vector of the fault-tolerant filter is then:

$$\overrightarrow{x} = \begin{bmatrix} \overrightarrow{x_1} \\ \overrightarrow{x_2} \\ \vdots \\ \overrightarrow{x_r} \\ \vdots \\ \overrightarrow{x_n} \\ \overrightarrow{D_1} \\ \overrightarrow{D_2} \\ \vdots \\ \overrightarrow{D_j} \\ \vdots \\ \overrightarrow{D_m} \end{bmatrix} \tag{6}$$

where there are n receivers and m satellites within the integrity monitor, and $\overrightarrow{D_j}$ is defined as the satellite clock and ephemeris errors:

$$\overrightarrow{D_j} = \begin{bmatrix} \zeta_j \\ \Delta\overrightarrow{\gamma}_j \end{bmatrix} \tag{7}$$

3. Integrity Information

The UREs and its' Error Bounds (standard deviations) can be obtained through the process of projecting the estimates of $\zeta^{(k)}$ and $\Delta\overrightarrow{\gamma}^{(k)}$ onto the Line-Of-Sight (LOS) of the potential user location.

The LOS vector from the position of the kth satellite, $\overrightarrow{x}^{(k)}_{sat}$, to a potential user location, $\overrightarrow{x}_{pos,u}$, is a unit vector:

$$\overrightarrow{l}_{k,u} = \frac{\left(\overrightarrow{x}^{(k)}_{sat} - \overrightarrow{x}_{pos,u}\right)}{|\overrightarrow{x}^{(k)}_{sat} - \overrightarrow{x}_{pos,u}|}$$

The UREs, $\beta_u^{(k)}$, at the position of u is therefore:

$$\beta_u^{(k)} = \begin{bmatrix} 1 \\ \overrightarrow{l}_{k,u} \end{bmatrix}^T \cdot \begin{bmatrix} \zeta^{(k)} \\ \Delta\overrightarrow{\gamma}^{(k)} \end{bmatrix} \tag{8}$$

Similarly, the standard deviation of $\beta_u^{(k)}$, $\sigma_u^{(k)}$, is obtained through the linear transformation of the projection:

$$\sigma_u^{(k)^2} = \begin{bmatrix} 1 \\ \overrightarrow{l}_{k,u} \end{bmatrix}^T \cdot COV\left(\begin{bmatrix} \zeta^{(k)} \\ \Delta\overrightarrow{\gamma}^{(k)} \end{bmatrix}\right) \cdot \begin{bmatrix} 1 \\ \overrightarrow{l}_{k,u} \end{bmatrix} \tag{9}$$

Here, we define the pair of $\beta_u^{(k)}$ and $\sigma_u^{(k)}$ as integrity information that the IMS is providing to the users. The PPP users receive the UREs and their Error Bounds of the GPS constellation as extra corrections in their pseudorange model.

Users can simply apply the corrections to the measurement models:

$$\tilde{\rho}_{\mathrm{IF},r}^{(k)} = \| \overrightarrow{x}_{sat}^{(k)} - \overrightarrow{x}_{pos,r} \| + \left(b_r - b_{sat}^{(k)} \right) + m_r^{(k)} \nabla \hat{T}_r + R_{\rho,r}^{(k)} + \beta_u^{(k)} + \epsilon_r^{(k)} \tag{10}$$

$$\tilde{\phi}_{\mathrm{IF},r}^{(k)} = \| \overrightarrow{x}_{sat}^{(k)} - \overrightarrow{x}_{pos,r} \| + \left(b_r - b_{sat}^{(k)} \right) + m_r^{(k)} \nabla \hat{T}_r + A^{(k)} + R_{\phi,r}^{(k)} + \beta_u^{(k)} + \epsilon_r^{(k)} \tag{11}$$

The associated measurement noise is also inflated with the uncertainty of the UREs:

$$R_{\tilde{\rho}_{\mathrm{IF},r}^{(k)}} = R_{\rho_{\mathrm{IF},r}^{(k)}} + {\sigma_u^{(k)}}^2 \tag{12}$$

$$R_{\tilde{\phi}_{\mathrm{IF},r}^{(k)}} = R_{\phi_{\mathrm{IF},r}^{(k)}} + {\sigma_u^{(k)}}^2 \tag{13}$$

4. Protection Level

Given that any potential satellite clock or ephemeris faults are protected by the integrity information, the protection level is simply the constant multiple of user position sigma.

$$PL_e = K \cdot \sigma_e \tag{14}$$

$$K = Q^{-1}\left(1 - \frac{PHMI}{2}\right) \tag{15}$$

where PL_e is the protection level in e direction (i.e. vertical or horizontal), σ_e is the 1-sigma uncertainty of position estimates from the user filter, Q is CDF of normal distribution and PHMI is Probability of Hazardously Misleading Information. PHMI is assumed to be 10^{-7} in this paper.

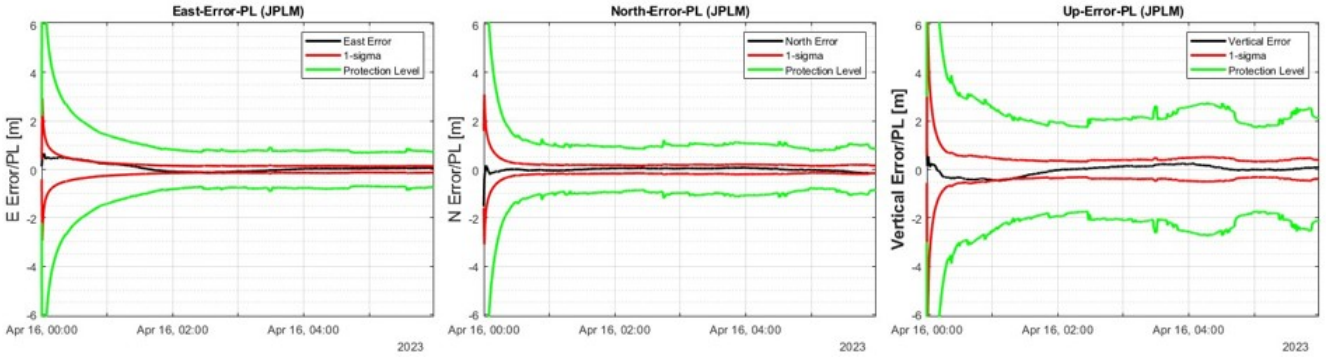

Figure 1: Performance of JPLM user.

Fig.1 is the performance of a PPP user at JPLM station with integrity information provided by the 56-station network introduced in Fig.2. It includes the position errors in East-North-Up directions, 1-sigma position uncertainties and the associated protection levels. The protection levels are simply the constant multiples of the user's 1-sigma uncertainties.

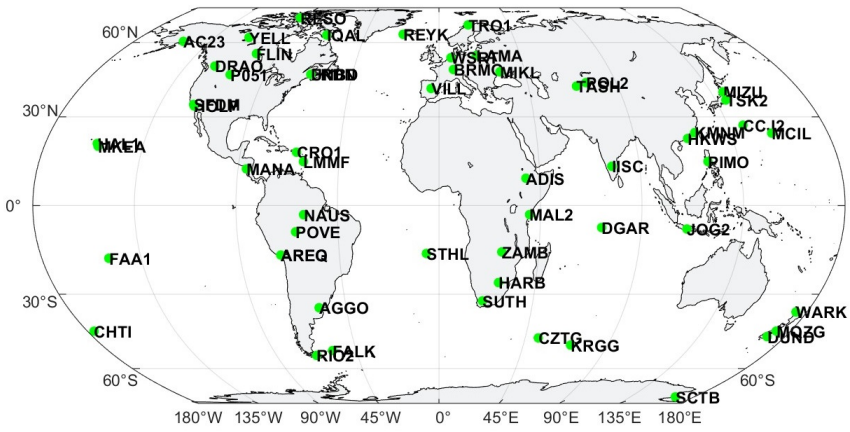

Figure 2: 56 selected IGS stations.

5. Information Form of Steady-State Satellite Errors

It is derived in Lai et al. (2026) that the covariance of the satellite errors at steady-state can be represented as:

$$Y_{sat} = \Sigma_{sat}^{-1} \tag{16}$$

$$\begin{aligned} Y_{sat} = Q_{sat}^{-1} + \sum_{r=1}^{n} C_{sat,r}^{T} \left(C_{rcv,r} Q_{rcv,r} C_{rcv,r}^{T} + R_r \right)^{-1} C_{sat,r} \\ + C_{sat,const}^{T} R_{const}^{-1} C_{sat,const} \end{aligned} \tag{17}$$

where $C_{sat,r}$, $C_{rcv,r}$, R_r correspond to the measurement models and noise of each receiver respectively and independently. $C_{sat,const}$ and R_{const}^{-1} are the zero-mean constraint described in Lai et al. (2024).

Eq.17 computes the information matrix of the satellite error by summing over the contributions of each receiver with their LOS satellites, and finally a matrix inversion to convert the information matrix into covariance that enables the projection to URE. Each receiver would be LOS to $\sim$10s satellites at a time, meaning its relatively lightweight in terms of matrix computation, and the final matrix inversion will have a fix dimensionality of $m \cdot 4$ that only requires to be computed 1 time. This allows extremely efficient evaluation of the steady-state satellite error covariance regardless of the number of total receivers within the network.

Consequently, Fig.3 is the steady-state VPL map of 99% availability on April 16th with the network specified in Fig.2, where the integrity information is computed from Eq.17. The LOS vectors are constructed from the GPS almanac. This is the performance of the 56 selected IGS station network for users within the integrity monitor network.

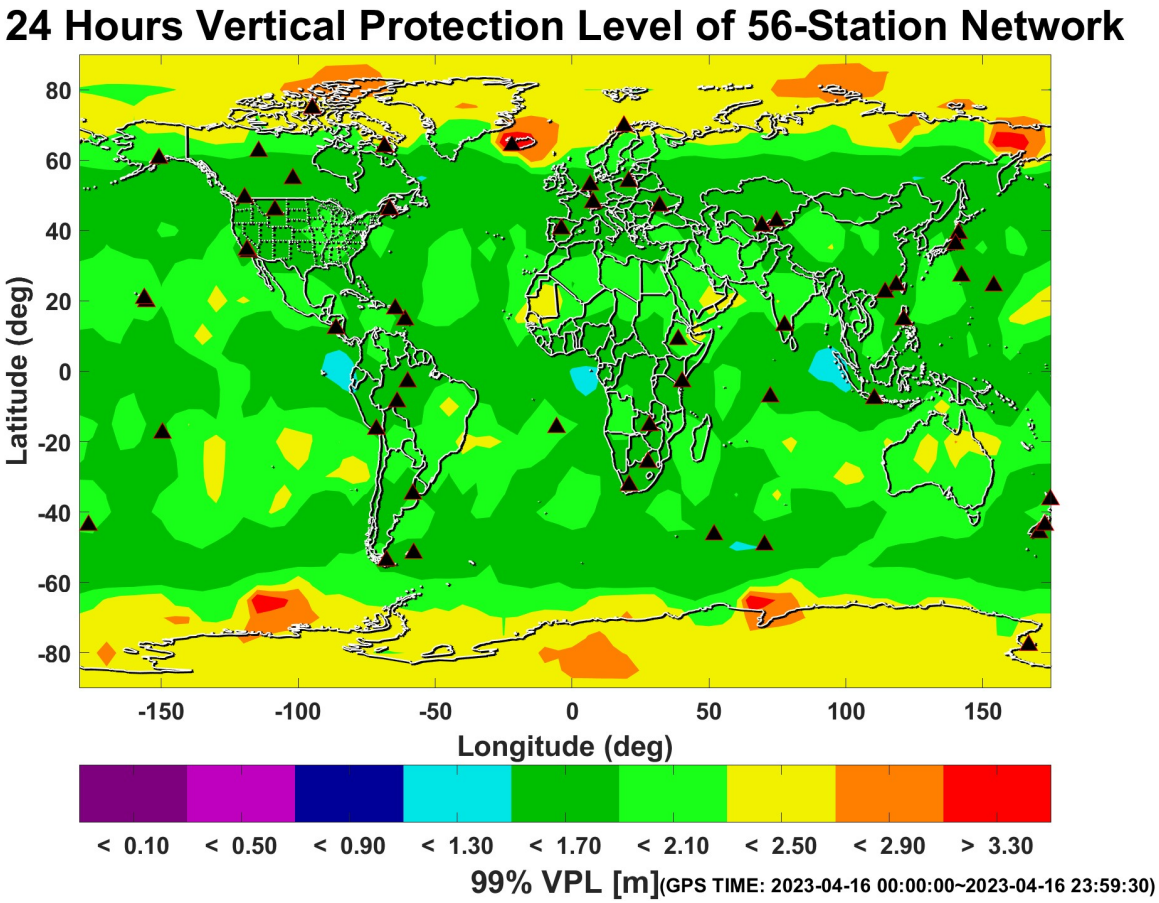

Figure 3: 99% Availability Steady-State VPL from Almanac.

III. RECEIVER DESIGN VIA CONVEX OPTIMIZATION

In the scale of the earth, the placement of the receivers is not sensitive to its exact location. Displacements on the order of tens to few hundreds of kilometers do not appear to introduce significant differences in the performance of the integrity monitor. Therefore, the placement of the receivers for the integrity monitor can be approximated with the selection from a pool of potential available receivers.

Mathematically, the problem can be formulated as the selection of K receivers from N candidate receivers.

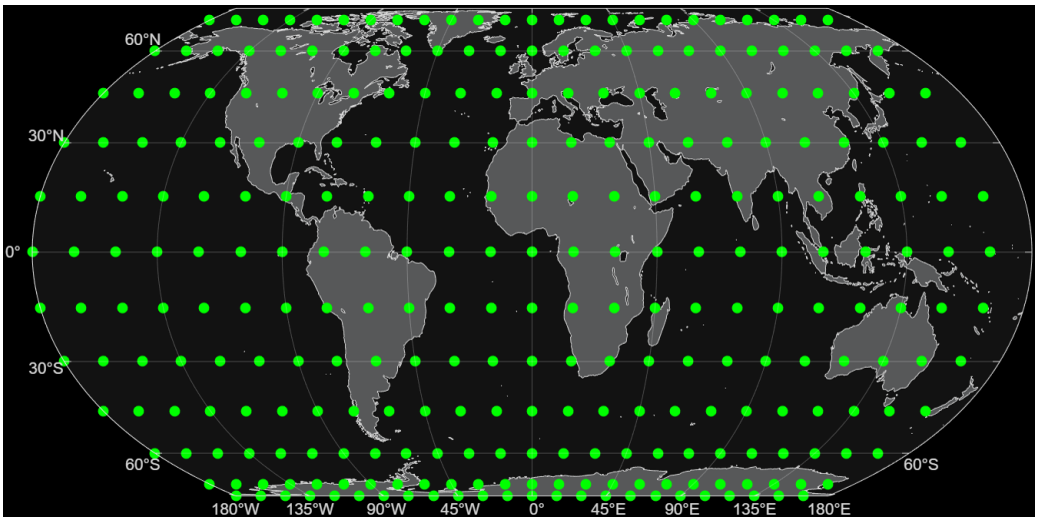

Figure 4: $5^\circ \times 5^\circ$ Global Grids.

For instance, for a global network size of 60 receivers, one can determine where to put the receivers by selecting 60 out of all the possible receivers locations shown in Fig.4, that is consists of grids points every 5 degrees in latitude and longitude. Ignoring the fact that some part of the grid parts might be infeasible to place receiver for now.

The naive way of placing the 60 receivers is iterate through all the combinations possible with the candidate receivers, then compare the performance of each of the combination as illustrated in Lai et al. (2026) until the resulting protection levels satisfy the requirement. This would involve evaluating $\binom{N}{k}$ combinations. In this example the actual number would be $\binom{312}{60}$. Unfortunately, it is computationally infeasible to be numerated in today's computer structure.

In terms of the number of receivers, one principle is that the more receivers used in a network, the better the performance of the network will be. Ignoring the possibility of faulted receivers, the overall information will only increase as the number of the receivers increase. In the most extreme scenario, if the performance of the network does not satisfy the requirement after iterating through all $\binom{312}{60}$ combinations, such as the protection level of certain locations are not low enough, the number of the candidate receivers can be increased by 1, and re-evaluate the whole $\binom{312}{61}$ until the performance is satisfied. Similarly, the number of the receivers can also be decreased to reduce the load of the network while the desired network performance is met. Since the number of receivers are always integer, it could be determined incrementally or decrementally by a fixed value.

Although the naive solution of placing the receivers is not feasible, instead of trying to place the receivers on the map, the more systematic way of doing it is first identifying all the possible location of the receivers for the network, then choose a certain number out of them. This is the main methodology behind the design of the receivers for the ground-based integrity monitor in this thesis. One can always adds more candidate receivers to increase the available combinations, but as mention earlier, at the scale of the GNSS constellation, the LOS difference are rather insensitive in terms of absolute distances between the receivers.

1. Selection As Convex Optimization:

Recall the steady-state information form of the satellite errors from Eq.17, an initial form of receiver selection via convex optimization can be written as a form of sensor selection shown in Joshi and Boyd (2008):

$$
\begin{aligned}
&\text{maximize} \quad \textbf{obj.} \\
&\text{s.t.} \quad Y_{sat} = Q_{sat}^{-1} \\
&\qquad + \sum_{r=1}^{n} \mathbf{Z}_r \cdot C_{sat,r}^T \left(C_{rcv,r} Q_{rcv,r} C_{rcv,r}^T + R_r \right)^{-1} C_{sat,r} \\
&\qquad + C_{sat,const}^T R_{const}^{-1} C_{sat,const} \\
&\qquad , 0 \leq \mathbf{z}_r \leq 1 \; \forall \; r \in \{0, 1, \ldots, n-1\} \\
&\qquad , \mathbf{1}^T \cdot \mathbf{Z}_r = k
\end{aligned}
\tag{18}
$$

where **obj.** is the objective of the optimization problem and is not specified for now, $\mathbf{Z}_r = [\mathbf{z}_0, \mathbf{z}_1, \ldots, \mathbf{z}_{n-1}]^T \in R^{n\times 1}$ is the floating point relaxation of the indicator for the receiver selection ranges from 0 to 1. $\mathbf{Z}_r$ is also the design variables for the problem. It controls the contribution of a receiver towards the information matrix of the satellite errors at steady-state from the receiver network, where there are a total of k receivers to be chosen from n receivers. Y_{sat} is the information matrix of the satellite errors with fractional information contribution from each of the receivers.

Eq.18 describes the relations of the satellite errors with all the potential receivers to be selected, that is universal regardless the choice of the design for the problem. However, the objective function is to some extent arbitrary depending on the requirements. Since the overall goal of the integrity network is to have as small protection level as possible, a straightforward choice of the objective function for the the problem would simply be minimizing the protection levels at the target user locations. Unfortunately, the position covariance to be used to compute the protection levels involves solving ARE, which includes non-convex operation such as matrix inversion. Although the ARE can be relaxed with schur-complement, there is no guarantee for this relations to be met given the freedom of inequalities from the schur-complement. Moreover, the formulation of schur-complement makes the problem cumbersome and heavily deteriorate the numerical stability of the solver. Only a small scale set of receiver selection can be solved reliably with the numerical solver. In general, any attempt to perform matrix inversion with the convex relaxation of schur-complement is numerically demanding. The dimensionality and the number of variables must be kept small for the problem to be solved numerically. As a result, instead of directly optimizing the protection levels, the goal is to minimize the measurement noise associated with the users.

Since the sigmas of the UREs from the integrity information are direct addition to the measurement noise of the user filter as shown in Eq.12 and 13.

The minimal protection levels the users can achieve is when the sigmas approach zero:

$$\sigma_u^{(k)} \to 0$$

Therefore, minimizing $\sigma_u^{(k)}$ is proportional to minimizing the protection levels.

To avoid the numerical instability from the Schur-complement, the goal here is to minimize the sigmas of the UREs from the information matrix.

Given the vector $B_{u,k} = [1 \ \overrightarrow{e}_{u,k}^T]^T$ that projects the satellite clock and ephemeris errors from the kth satellite to the user u, the same projection vectors on the covariance and information matrices are:

$$\sigma_u^{(k)^2} = B_{u,k}^T \cdot \Sigma_{sat} \cdot B_{u,k} \tag{19}$$

$$\alpha_u^{(k)^2} = B_{u,k}^T \cdot Y_{sat} \cdot B_{u,k} \tag{20}$$

where $\sigma_u^{(k)}$ is the URE sigmas and $\alpha_u^{(k)}$ is the linear protection onto the information matrix that is loosely related to $\sigma_u^{(k)}$:

$$4 \cdot \frac{1}{\kappa} \leq \sigma_u^{(k)^2} \cdot \alpha_u^{(k)^2} \leq 4 \cdot \kappa \tag{27}$$

Eq.27 can be shown as follow.

κ is the condition number of the covariance matrix Σ_{sat}.

$$\kappa = \frac{\lambda_{max}\left(\Sigma_{sat}\right)}{\lambda_{min}\left(\Sigma_{sat}\right)} \tag{21}$$

Since

$$\sigma_u^{(k)^2} \cdot \alpha_u^{(k)^2} = B_{u,k}^T \cdot \Sigma_{sat} \cdot B_{u,k} \cdot B_{u,k}^T \cdot Y_{sat} \cdot B_{u,k} \tag{22}$$

and

$$\Sigma_{sat} = Y_{sat}^{-1} \tag{23}$$

Given

$$\lambda_{min}\left(B_{u,k}^T \cdot \Sigma_{sat} \cdot B_{u,k}\right) \leq B_{u,k}^T \cdot \Sigma_{sat} \cdot B_{u,k} \leq \lambda_{max}\left(B_{u,k}^T \cdot \Sigma_{sat} \cdot B_{u,k}\right) \tag{24}$$
$$\lambda_{min}\left(B_{u,k}^T \cdot\ Y_{sat} \cdot B_{u,k}\right) \leq B_{u,k}^T \cdot\ Y_{sat} \cdot B_{u,k} \leq \lambda_{max}\left(B_{u,k}^T \cdot\ Y_{sat} \cdot B_{u,k}\right)$$

where $B_{u,k}$ is the linear projection of the clock and ephemeris error to the range domain, and would at most contributes to the multiple of a constant 2 due to the projection of the satellite clock bias and ephemeris error by LOS vector. Eq.24 becomes:

$$2 \cdot \lambda_{min}\left(\Sigma_{sat}\right) \leq B_{u,k}^T \cdot \Sigma_{sat} \cdot B_{u,k} \leq 2 \cdot \lambda_{max}\left(\Sigma_{sat}\right)$$
$$2 \cdot \lambda_{min}\left(Y_{sat}\right) \leq B_{u,k}^T \cdot\ Y_{sat} \cdot B_{u,k} \leq 2 \cdot \lambda_{max}\left(Y_{sat}\right) \tag{25}$$

Since $\lambda_{min}\left(\Sigma_{sat}\right) = \frac{1}{\lambda_{max}(Y_{sat})}$ and $\lambda_{max}\left(\Sigma_{sat}\right) = \frac{1}{\lambda_{min}(Y_{sat})}$, Eq. 25 becomes:

$$2 \cdot \lambda_{min}\left(\Sigma_{sat}\right) \leq B_{u,k}^T \cdot \Sigma_{sat} \cdot B_{u,k} \leq 2 \cdot \lambda_{max}\left(\Sigma_{sat}\right)$$
$$2 \cdot \frac{1}{\lambda_{max}\left(\Sigma_{sat}\right)} \leq B_{u,k}^T \cdot\ Y_{sat} \cdot B_{u,k} \leq 2 \cdot \frac{1}{\lambda_{min}\left(\Sigma_{sat}\right)} \tag{26}$$

Therefore, the product in Eq. 22 is bounded by the condition number of $\Sigma_u^{(k)}$:

$$4 \cdot \frac{1}{\kappa} \leq C_{u,k} \leq 4 \cdot \kappa \tag{27}$$

where

$$\sigma_u^{(k)^2} \cdot \alpha_u^{(k)^2} = C_{u,k} \tag{28}$$

Thus, $\alpha_u^{(k)^2}$ is the reciprocal of the URE variance with a multiplier that is bounded by the condition number of $\Sigma_u^{(k)}$.

Additionally,

$$\alpha_u^{(k)^2} = \frac{C_{u,k}}{\sigma_u^{(k)^2}}$$

That is, maximizing $\alpha_u^{(k)^2}$ is therefore equivalent to minimizing the URE variance, $\sigma_u^{(k)^2}$, weighted by the positive $C_{u,k}$ that is bounded by the condition number of $\Sigma_u^{(k)}$, and is equivalent to minimizing the protection levels for the users.

Since the condition number of the outer product of the projection vector, is composed of the LOS vector given the geometry between the satellites and the users, the satellites with better geometry with the users will generally have LOS more well-conditioned. As a result, $C_{u,k}$ weights more on the satellites that have poor geometry with the users, which are exactly the satellites that would contribute to poorer protection levels for the users.

The process of receiver selections can thereby be formulated as a complete convex optimization problem.

$$\begin{aligned}
\text{maximize} \quad & \min\{\alpha_{u,t}^{(k)^2}\} \\
\text{s.t.} \quad & Y_{sat,t} = Q_{sat,t}^{-1} \\
& + \sum_{r=1}^{n} \mathbf{Z}_r \cdot C_{sat,r}^T \left(C_{rcv,r,t} Q_{rcv,r,t} C_{rcv,r,t}^T + R_r\right)^{-1} C_{sat,r,t} \\
& + C_{sat,const,t}^T R_{const}^{-1} C_{sat,const,t} \\
& , 0 \leq \mathbf{z}_r \leq 1 \ \forall\ r \in \{0, 1, \ldots, n-1\} \\
& , \mathbf{1}^T \cdot \mathbf{Z}_r = k,\ \mathbf{Z}_r = [\mathbf{z}_1, \cdots, \mathbf{z}_n]^T \\
& , \alpha_{u,t}^{(k)^2} = B_{u,k,t}^T \cdot Y_{sat,t} \cdot B_{u,k,t}
\end{aligned} \tag{29}$$

where the objective to be maximized is the minimal of the weighted reciprocal of the projected URE variance at the location of the target user u at time t. The maximization process connects the projection of the URE variance with different time steps over a period of time such that the receivers selected include the temporal relations of the satellite ephemeris. Finally, the receivers with the top k values of $\mathbf{z}_r$ are selected to be the network receivers.

IV. EPHEMERIS DATA

No real observation data and precise product are used in this paper. Only the GPS almanac data is used generate the the LOS information. In particular, the ephemeris from the almanac data allows quick evaluation of the receiver to satellite geometry and the covariance computation when combine with Eq.17. This is inspired by Jan et al. (2009).

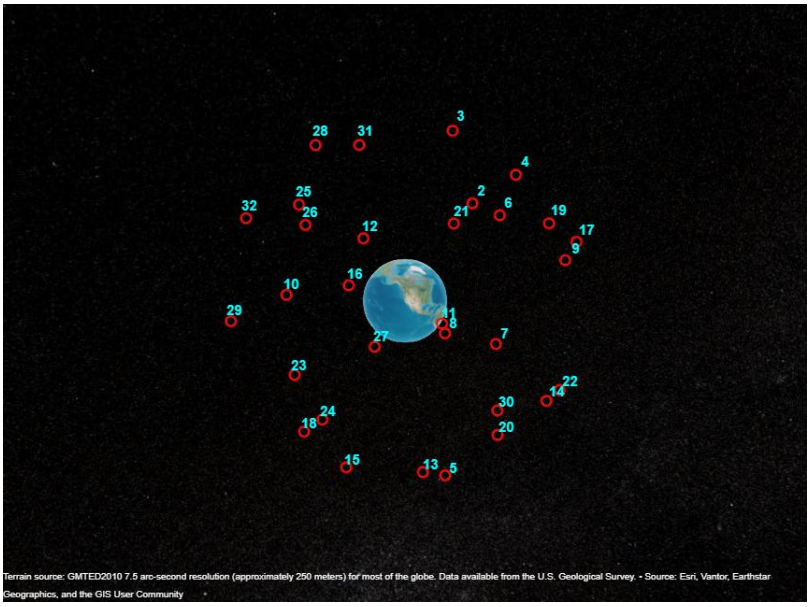

Figure 5: Ephemeris simulation from almanac.

where Fig.5 shows a snapshot of the ephemeris simulation of GPS constellation from the almanac. The red circles are the satellites with the numbers representing the corresponding PRN. The almanac provides the ephemeris in ECEF coordinate using coarse Keplerian orbit model. The accuracy of such orbits is at the scale of $\sim$1 km compare with the precise product. It is not accurate enough for state estimation given the kilometer level of pseudorange errors, but good enough for the approximations of LOS vector and elevation angle, for which the modeling error of $\sim$1 km is normalized by the GPS orbital altitude of $\sim$20200 km. As a result, the almanac itself is suitable for the simulation of the covariance estimates as well as the computation of the protection levels.

Given the location of the receivers from the integrity monitor, we can then simulate the LOS vectors from the almanac with the elevation angles as the cut-off criteria. To some degree, the protection levels computed from such simulation represent the lower bound of the protection levels that the geometry of the integrity monitor can achieve. In terms of the LOS vectors, the almanac will always be more stable than the actual receivers, which might have events such as cycle slips, loss of track, or multi-path etc. that would degrade the available satellites for the receiver. Even though the LOS vectors from the precise product and almanac are almost identical, the covariance computed from the actual receivers will be greater than or at least equal to the one computed from the almanac given that the only cut-off criteria for the almanac are elevation angle.

V. SELECTION RESULT

This section demonstrate the results of selecting 56 stations out of the candidate receivers for the integrity network by maximizing the objective and constraints specified in Eq.29. The constraint optimization problem is solved in Matlab using CVX, a package for specifying and solving convex programs CVX Research (2012)Grant and Boyd (2008).

1. Evenly Spread Candidate Receivers

The pool of candidate receivers are subject to the designer of the network. They represent the locations where reference stations are feasible to be placed and operated for the integrity monitor.

As shown in Fig.4, while the $5^\circ \times 5^\circ$ global grids provides the full coverage to the surface of the earth for the candidate receivers, the spacing between the receivers are not uniform due to the curvature of the earth. The candidate receivers are concentrated in higher latitude, creating inefficient distribution that does not fully capture the spatial geometries of the potential network during the optimization process.

Therefore, in this example, 56 stations are selected from a pool of 200 candidate receivers that are evenly spread-out across the surface of the earth. The spatially uniform candidate receivers are shown in Fig.6 and their locations are generated using uniform sampling technique (Semechko, 2026), where the random seed is set to 1 to ensure the distribution is deterministic throughout the optimization. Whether the receivers are physically possible to be placed at the candidate locations are ignored for now. The objective of this example is to demonstrate the optimal design of a global network by efficiently selecting from the $\binom{200}{56}$ possible combinations via convex optimization.

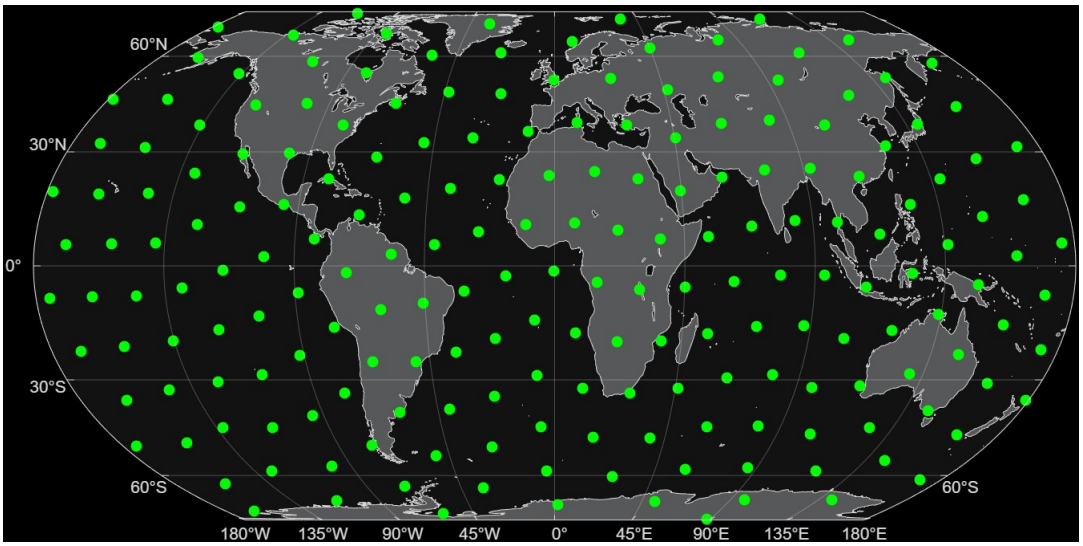

Figure 6: 200 evenly spread-out candidate receivers.

In addition to determining the candidate receivers, the target user locations must also be specified in the actual optimization problem. The user locations are the point where the satellite errors are projected to. Essentially, Eq.29 is only minimizing the protection levels of the user locations that are specified by $B_{u,k,t}$, where a predetermined user location is required to do the projections. Therefore, depending on the targeting area of service, for instance, a similar evenly distributed locations can be used as the target users when the goal is to equally minimizing the protection levels around the world. Alternatively, the target users can be specified based on the service requirements that could be locally concentrated to specific regions. In this example, a global service is desired so 80 evenly spread-out target users are adopted.

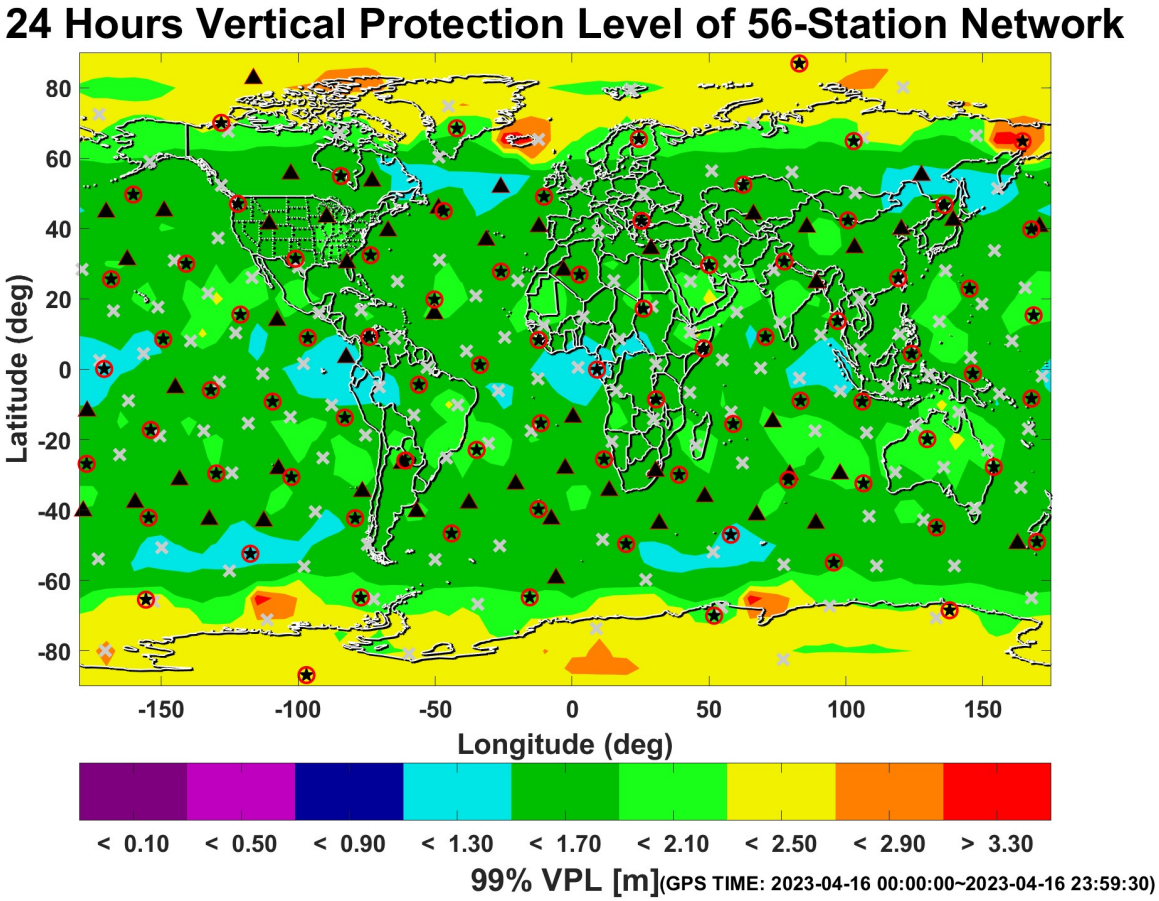

Figure 7: Evenly spread-out Receiver Selections

Fig.7 shows the VPLs of 99% availability of the network size of 56 receivers chosen from solving 29. There are 200 uniformly distributed candidate receivers and 80 uniformly distributed target users in the problem. The black astroid within the red circles represent the target users, the black triangles are the 56 receivers selected, and the gray crosses are the other 144 receivers that are not selected by the optimization process. The network is obtained by optimizing over the period of 24 hours with 10 minutes interval using ephemeris data on April 16th.

In comparison with Fig.3, the VPLs are generally smaller than the original 56-station network as shown in Fig.7. Without changing the number of the receivers within the network, the selection results gives the new geometries of the receiver network that can provide smaller protection levels than the old design when ignoring the temporal effects.

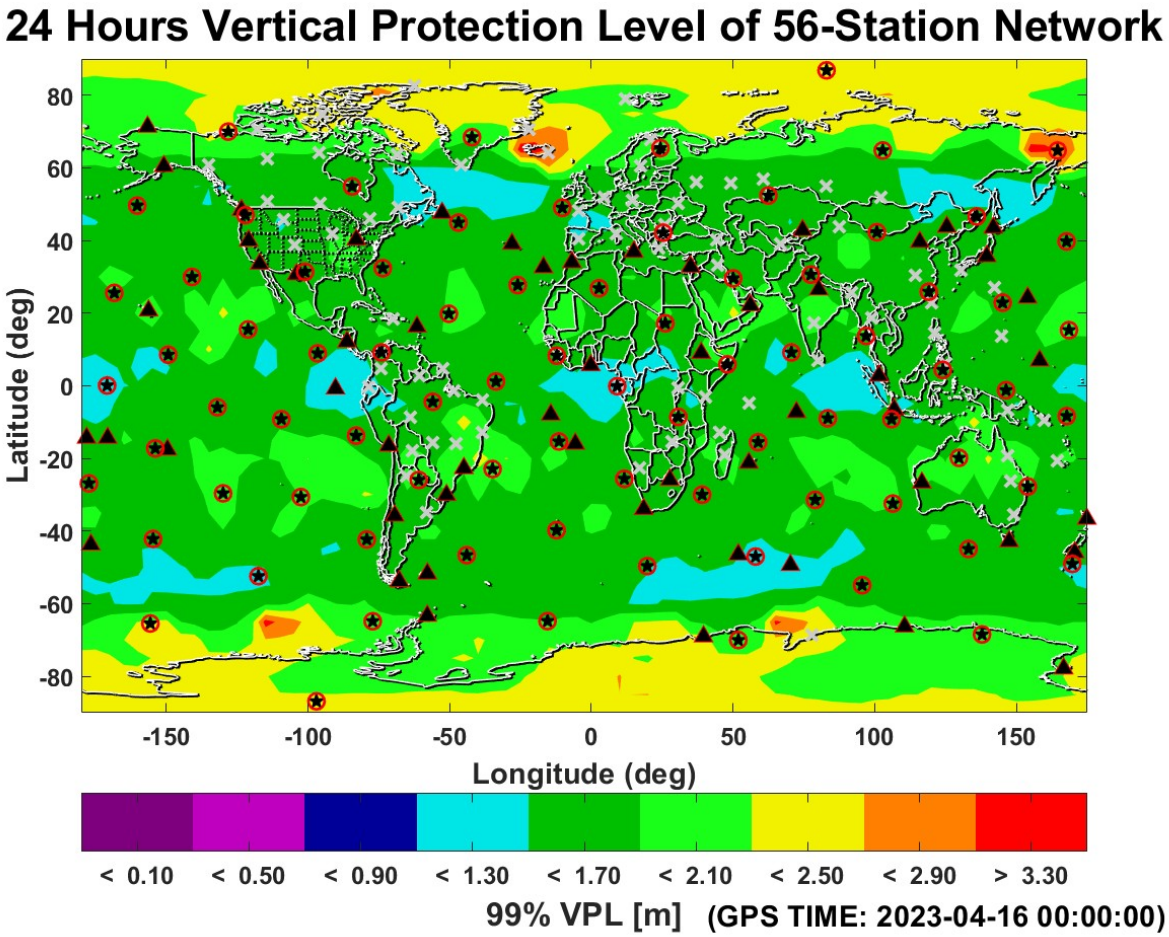

Figure 8: IGS Network Receiver Selections

Similarly, Fig. 8 shows the selection results that the candidate receiver locations are belong to the IGS network. The selected locations are physically feasible to place antennas and receivers. This new 56-station IGS network exhibits similar performance as Fig. 7 after selecting by the convex optimization process.

2. Receiver Number Determination

The determination of the number of receivers becomes straightforward once the process for determining receiver locations is streamlined. The more receivers included in the network, the more information is collected, resulting in better performance.

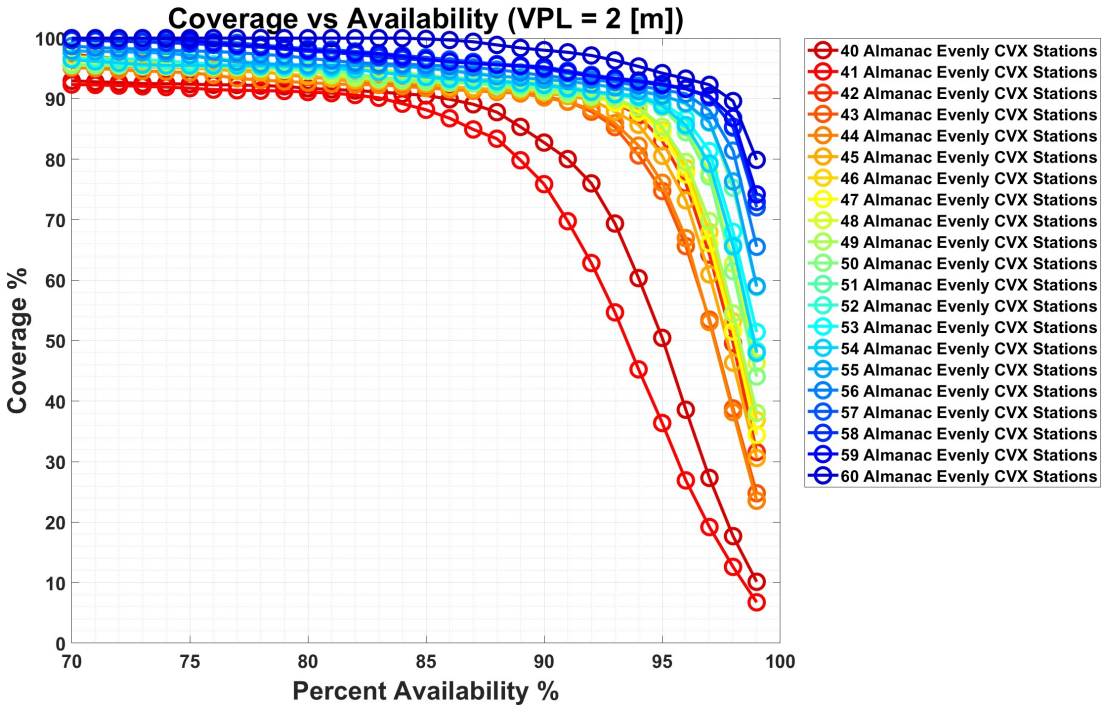

Figure 9: Coverage vs. Availability for evenly spread-out network with receiver number ranges $40 \sim 60$.

Fig.9 illustrate this principal, where the 200 and 80 evenly spread-out candidate receivers and target users are re-used as a demonstration. The coverage vs. availability with a 2 m threshold indicates the percentage of the surface of the Earth that has VPL less than 2 m. Each availability represents a lower quantile of global VPL distribution.

The only variable here is the number of desired receivers, k in Eq.29. Each line is the solution from the solving the same convex optimization problem, but with different k values ranges from 40 to 60, representing the size of the desired network. It can be seen that the more receivers are used, the better the coverage of the network.

Thus, the process of determining the receiver number can do done by simply enumerating the solutions from a range of acceptable numbers, and choose the one that satisfy the requirement. Since the cost and the probability of receiver failure increases along with the number of receiver, this becomes a trad-off between the performance (the more the better), and operational limit (the less the better), which depend on the design requirement.

The solutions of Eq.29 with different receiver number, k, may not strictly monotonically increasing due to the relaxation of the integer constraints, but as shown in Fig.9, the performance of the network is positively related to the number of receivers.

One can always add additional receivers to an existing network, which guarantees monotonically increasing performance. However, this heuristic approach may lead to suboptimal performance as more receivers are added due to the incremental extension of a pre-existing network.

VI. CONCLUSION

In this paper, we developed a method that uses convex optimization method to optimally design the locations of the receivers while indirectly minimizing the protection levels of the target users. The resulting design of the network has shown relatively lower protection levels than the 56 IGS station network, given the same number of receivers. Depending on the interested area and the available regions to place receiver, the designer can easily determine the optimal geometries of the network that can minimize the protection levels for the users. To determine the number of required receivers, one simply needs to incrementally or decrementally varying the desired network size, and choose the one that satisfy the requirement given the protection level map.

ACKNOWLEDGEMENTS

We gratefully acknowledge the support of the FAA Satellite Navigation Team for funding this work under Memorandum of Agreement #: 693KA8-22-N-00015.

REFERENCES

CVX Research, I. (2012). CVX: Matlab software for disciplined convex programming, version 2.0. https://cvxr.com/cvx.

Grant, M. and Boyd, S. (2008). Graph implementations for nonsmooth convex programs. In Blondel, V., Boyd, S., and Kimura, H., editors, *Recent Advances in Learning and Control*, Lecture Notes in Control and Information Sciences, pages 95–110. Springer-Verlag Limited. http://stanford.edu/~boyd/graph_dcp.html.

Jan, S.-S., Chan, W., and Walter, T. (2009). Matlab algorithm availability simulation tool. *GPS solutions*, 13(4):327–332.

Joshi, S. and Boyd, S. (2008). Sensor selection via convex optimization. *IEEE Transactions on Signal Processing*, 57(2):451–462.

Lai, Y.-F., Blanch, J., and Walter, T. (2024). Ground-based integrity monitors for ppp correction services. In *Proceedings of the ION 2024 Pacific PNT Meeting*, pages 514–526.

Lai, Y.-F., Blanch, J., and Walter, T. (2026). Performance evaluation for ground-based integrity monitor network. In *Proceedings of the ION 2026 Pacific PNT Meeting*, pages 272–285.

Semechko, A. (2026). Suite of functions to perform uniform sampling of a sphere. https://github.com/AntonSemechko/S2-Sampling-Toolbox. Retrieved May 10, 2026.

Welch, G., Bishop, G., et al. (1995). An introduction to the kalman filter.

Zumberge, J., Heflin, M., Jefferson, D., Watkins, M., and Webb, F. H. (1997). Precise point positioning for the efficient and robust analysis of gps data from large networks. *Journal of geophysical research: solid earth*, 102(B3):5005–5017.